THE JOURNAL OF PHYSICAL CHEMISTRY C

Article

pubs.acs.org/JPCC

Correlating Surface-Functionalization of Mesoporous Silica with Adsorption and Release of Pharmaceutical Guest Species

Victoria Morales,[†] Matthew N. Idso,[‡] Moisés Balabasquer,[†] Bradley Chmelka,*[,‡] and Rafael A. García-Muñoz*[,†]

[†]Group of Chemical and Environmental Engineering, ESCET, Rey Juan Carlos University. C/Tulipán s/n, 28933 Móstoles, Madrid, Spain

[‡]Department of Chemical Engineering, University of California at Santa Barbara, Santa Barbara, California 93106, United States

Supporting Information

ABSTRACT: We present here a detailed molecular-level understanding of the interactions among surface-functionalized mesoporous SBA-15 silica and pharmaceutical guests that influence macroscopic adsorption and release behaviors. A model drug species, methylprednisolone sodium succinate, was adsorbed on the surfaces of functionalized mesoporous SBA-15 silica materials with different aminoalkyl species and without or with C_{60} fullerene moieties. Zeta potential measurements show that the electrostatic interactions among methylprednisolone species and modified silica surfaces are important for the adsorption and release of the methylprednisolone molecules. Complementary one and two-dimensional (2D) solid-state $^{13}C\{^1H\}$ NMR measurements provide evidence for specific intermolecular interactions between adsorbed methylprednisolone species and different types of functionalized silica surfaces. In particular, correlated ^{13}C and ^1H signal intensities from the methylprednisolone alkyl moieties and the aminoalkyl groups of the functionalized silica surfaces unambiguously establish their close (<1 nm) molecular proximities and strong interactions. The molecular-level insights are correlated with macroscopic adsorption and release behaviors of methylprednisolone, providing detailed new understanding of the interactions responsible for the high loadings and slow release of this important pharmaceutical agent from surface-functionalized mesoporous materials.

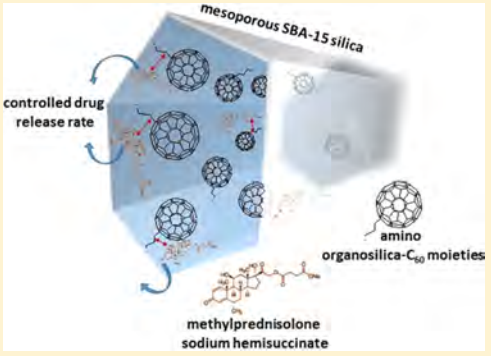

INTRODUCTION

The biocompatibilities, robustness, high specific surface areas, and facile surface functionalization of mesoporous silicas make these materials promising for applications in drug delivery.[1,2] Drug delivery systems (DDSs) aim to improve therapeutic efficacies and prevent the overdoses of pharmaceutical species by providing site-specific delivery of pharmaceuticals at controlled rates within the body. An additional objective for DDSs is to increase patient compliance by reducing the frequency of doses during the course of treatment, which is achieved by extending the duration over which DDSs deliver effective quantities of pharmaceuticals. Consequently, DDSs are engineered to maximize the adsorption capacities and control the release of pharmaceutical species under biological conditions (e.g., in the bloodstream, sinuses, etc.). Mesoporous silicas are promising as DDSs, because their high surface areas enable large pharmaceutical adsorption capacities and the robust silica frameworks render chemical and mechanical stability under biological conditions. By comparison, the relatively large (2−30 nm) pore sizes of mesoporous silicas allow pharmaceutical guests of large sizes to access the interior mesoporous surfaces. Furthermore, both the internal mesochannel and external particle surfaces of mesoporous silicas can be functionalized with a variety of pharmaceutically inactive chemical moieties that interact with molecular guests and thereby influence the adsorption and release properties of guest species.[3−5] Combined with the large pores, high surface areas and biocompatibilities, the ability to easily adjust material properties by surface functionalization enables mesoporous silicas to be highly effective DDSs for a variety of chemically distinct pharmaceuticals.

Functionalities at mesoporous silica surfaces can promote the adsorption of molecular guests to enable a variety of technological applications and are especially relevant in mesoporous silica-based drug delivery systems. In most cases, the adsorption of molecular guests to mesoporous silica surfaces involves hydrophobic, hydrogen-bonding, electrostatic, or covalent interactions among the guests and moieties at the silica surface. The strengths and extents of these distinct intermolecular interactions depend on the types and compositions of the surface functional groups, which significantly influence the chemical activities, acid−base properties, and hydrophobicities[6−14] of mesoporous silicas. For example, mesoporous silica grafted with alkyl, haloalkyl, or aryl moieties exhibit increased surface hydrophobicity compared to nonfunctionalized mesoporous silica.[15−18] Such

Received: June 20, 2016
Revised: June 28, 2016
Published: June 29, 2016

DOI: 10.1021/acs.jpcc.6b06238
J. Phys. Chem. C 2016, 120, 16887−16898

hydrophobic materials enable enhanced chromatographic performance when used as the stationary phase in reverse-phase high performance liquid chromatography columns, relative to commonly used silica gels.[19] By comparison, hydrophilic nonfunctionalized mesoporous SBA-15 silicas have high concentrations of surface silanol groups that interact with ibuprofen species by hydrogen-bonding, enabling high quantities of these pharmaceutical molecules to be adsorbed to such nonfunctionalized mesoporous silica surfaces.[20] Covalent interactions also result in the strong adsorption of guest molecules to functionalized mesoporous silicas and can facilitate the capture of dilute radionuclide,[21] boron,[22] or ibuprofen[23] species from solution by functionalized mesoporous materials. Molecular adsorption can also be influenced by electrostatic interactions, which enable the high adsorption capacities of poorly water-soluble prednisolone species to polyethylenimine-functionalized mesoporous silica materials.[24]

The release rates of pharmaceutical guests from mesoporous silica materials are strongly influenced by adsorption behaviors of the guest species near surface functional groups, which are mediated by site-specific molecular interactions. Specifically, slower transport of molecular species within silica mesochannels can result from adsorption interactions and steric effects between the guest species and surface moieties. Moreover, molecular release rates can also be influenced by the hydrophobicities of the mesoporous materials, which determine the rates at which aqueous biological media (e.g., blood) partition into materials and subsequently solubilize molecular guests. As a result, several previous studies have relied on modifying mesoporous materials with hydrophobic and/or bulky surface groups to control molecular release. Mesoporous SBA-15 silica materials functionalized with octyl or octadecyl groups exhibit erythromycin release rates that are 1 order of magnitude lower than from mesoporous silicas without surface functionalization.[25] Similarly, slow release rates have been reported for captopril[26] and ibuprofen[27] from mesoporous silicas with high degrees of surface silylation, which yields high surface hydrophobicities and correspondingly strong adsorption of pharmaceutical guests. Molecular simulations by Vallet-Regí and co-workers have suggested that a combination of electrostatic and hydrogen-bonding interactions are responsible for drug adsorption, desorption, and diffusion behaviors of pharmaceutical guests within surface-functionalized mesoporous silica hosts.[28,29] However, until now, direct molecular-level experimental measurements of such interactions and properties have been limited or absent.

The objective of this investigation is to understand the molecular interactions that mediate the adsorption and desorption of the pharmaceutical species methylprednisolone from the functionalized surfaces of mesoporous SBA-15 silicas to establish design criteria for controlled release applications. The incorporation of C_{60} into mesoporous silica materials is expected to yield a combination of hydrophobic, $\pi-\pi$, and steric interactions that enable high methylprednisolone adsorption capacities and reduced rates of macroscopic release. Functionalization of similar mesoporous MCM-41 materials with fullerene C_{60} species has been achieved by covalently attaching C_{60} species to grafted amino organosilica groups;[30] however, the resulting materials were not evaluated for the adsorption and release of pharmaceutical guests. Corticoids, including a variety that are synthetically manufactured, are commonly used for medicinal purposes because of their broad relevances in physiological processes, including regulation of stress and immune responses, inflammation, carbohydrate metabolism, protein catabolism, and blood electrolyte levels. The synthetic corticoid methylprednisolone was chosen as a representative pharmaceutical guest for this study, because it is often prescribed to treat a number of different health conditions including arthritis, sinusitis, bronchitis, and cancer.

The molecular interactions among adsorbed methylprednisolone guests and fullerene (e.g., C_{60}) functional groups at the mesoporous silica surfaces are established and correlated with methylprednisolone adsorption and release at the macroscopic level. The quantities of amino organosilica, HC_{60}, and methylprednisolone species incorporated into mesoporous SBA-15 silica hosts are established by using solid-state NMR spectroscopy, elemental analysis, and thermogravimetry, while the textural properties (i.e., surface areas, pore sizes, etc.) of materials were obtained from N_2 adsorption analyses. Zeta potential values for bulk functionalized materials indicate electrostatic interactions among methylprednisolone guests and the silica surface, the magnitudes of which correlate qualitatively with methylprednisolone adsorption capacities. Moreover, hydrogen-bonding and hydrophobic interactions of adsorbed methylprednisolone species with groups at the mesoporous silica surface are manifested directly by one- and two-dimensional solid-state $^{13}C\{^1H\}$ NMR spectroscopy. Insights regarding these intermolecular interactions are correlated with and explain the macroscopic release rates of methylprednisolone from functionalized mesoporous silica hosts into simulated body fluids at neutral and acidic conditions, which correspond to biological environments of the bloodstream and proximate to tumors, respectively. The surface-functionalized mesoporous SBA-15 silica materials in this study show higher methylprednisolone adsorption capacities and exhibit substantially longer release times compared to other nonfunctionalized mesoporous silicas and zeolite materials.[31] This detailed understanding of C_{60}-functionalized mesoporous silica loaded with methylprednisolone guests at molecular and macroscopic levels provides new opportunities for designing mesoporous silica-based materials for controlled pharmaceutical release.

EXPERIMENTAL SECTION

Materials. *Synthesis of SBA-15-NH$_2$ Silica.* The synthesis of mesoporous SBA-15 silica materials was accomplished using the method described previously by Zhao et al.[32] Mesoporous SBA-15 silica materials functionalized with organosilica species were synthesized as follows: 2.0 g of calcined SBA-15 silica was held under vacuum (200 mbar) at a temperature of 150 °C overnight to eliminate residual water. Next, these materials were added to 250 mL of anhydrous toluene stored under a nitrogen atmosphere and the mixture was stirred for 30 min at 110 °C. Then, 5.6 mmol of an organosilica precursor, specifically 3-aminopropyl trimethoxysilane (APS) or 4-aminobutyl trimethoxysilane (ABS), was added to this mixture, and the resulting mixture was stirred at 110 °C for 24 h. The solids were washed twice with toluene and acetone, filtered, and then dried overnight under vacuum (200 mbar). SBA-15 materials with grafted amino organosilica species are collectively referred to as SBA-15-NH$_2$ materials, or as SBA-15-APS-NH$_2$ and SBA-15-ABS-NH$_2$ to reflect the type of organosilica incorporated.

Preparation of SBA-15-NH-C$_{60}$H Materials. A solution containing fulleride anion $[C_{60}]^-$ was prepared by mixing C_{60} fullerene (86 mg, 0.12 mmol) with tetrahexylammonium bromide (THAB, 261 mg, 0.60 mmol) in 32 mL of anhydrous

DOI: 10.1021/acs.jpcc.6b06238
J. Phys. Chem. C 2016, 120, 16887−16898

Scheme 1. Principal Steps and Intermediates Involved in the Preparation of SBA-15-NH-HC$_{60}$ Materials[a]

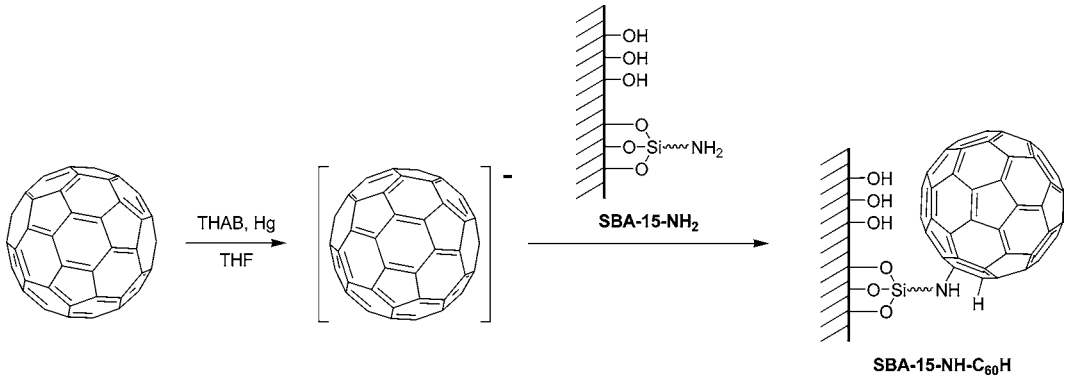

[a]Fulleride $[C_{60}]^-$ anions are formed as a product by mixing C_{60} fullerene species with THF in the presence of THAB and Hg (left arrow). This solution is exposed to the SBA-15-NH_2 materials (right arrow), which results in the covalent attachment of fulleride species to the primary amine groups of the amino organosilica species to yield SBA-15-NH-HC$_{60}$ materials.

tetrahydrofuran (THF) and 2−3 drops of mercury. The mixture was heated and maintained at 80 °C in a nitrogen atmosphere for 3 h after which the solution became dark red in color, which is the characteristic color of C_{60} radical ions. Subsequently, 400 mg of SBA-15-NH_2 was added to the solution containing C_{60} radical ions and the mixture stirred for 20 h under a nitrogen atmosphere. The solids were then filtered and then washed twice with toluene and acetone to remove unreacted C_{60} radical ions and THAB. Finally, these materials were dried under vacuum overnight to achieve the target materials. A schematic diagram of the C_{60} preparation and attachment procedure is shown in Scheme 1. Materials with C_{60} species are collectively termed SBA-15-NH-C_{60}H and individually named SBA-15-APS-C_{60}H, SBA-15-ABS-C_{60}H, and SBA-15-APhS-C_{60}H to reflect the propyl and butyl moieties of the incorporated organosilica species. Such C_{60}-functionalized mesoporous SBA-15 silica materials are expected to be nontoxic, based on the low cytotoxicities reported for fullerene-containing polymers in vitro,[33,34] the lack of acute toxicities for water-soluble fullerenes in vivo,[35] and the lack of cytotoxic or genotoxic effects for cancer cells exposed to aminopropyl-functionalized silica nanoparticles.[36]

Loading of Methylprednisolone Sodium Succinate onto SBA-15-Derived Silica. Methylprednisolone sodium succinate was loaded into the SBA-15, SBA-15-NH_2, and SBA-15-NH-C_{60}H materials by exposing materials to an aqueous solution containing dissolved methylprednisolone species. Specifically, SBA-15 or functionalized SBA-15 materials (200 mg) were added to an aqueous solution containing methylprednisolone at a concentration of either 15 or 50 mg mL^{-1}, and was stirred vigorously at room temperature for 24 h. The materials were filtered, washed and dried under vacuum at 70 °C overnight. As soaking materials in the 50 mg mL^{-1} methylprednisolone solution yielded the greater pharmaceutical loadings (data not shown here), materials used for drug release experiments were prepared using solutions at this concentration.

In Vitro Release of Methylprednisolone Sodium Succinate from SBA-15-Derived Silica. Sterilized dialysis bags (molecular-weight cutoff 10 000 Da) were pretreated prior to use by immersion into a boiling aqueous mixture of 50% ethanol (v/v) for 1 h. Then the dialysis bags were washed with water up to 40 °C for 1 h and then immersed in a simulated body fluid (SBF) at 37 °C for 2 h. For pharmaceutical release experiments at neutral conditions the SBF consisted of a phosphate buffered saline (PBS) solution (pH 7.4), while an acetate buffered solution (pH 4.6) was used for experiments under acidic conditions.

Methylprednisolone release from materials into SBF was monitored to understand pharmaceutical release properties of these materials. SBA-15, SBA-15-NH_2, or SBA-15-NH-C_{60}H material (100 mg) loaded with methylprednisolone species was dispersed into 2 mL of SBF. This suspension was subsequently added to a pretreated dialysis bag, which was sealed and placed into bottles containing 100 mL of SBF (referred to as release media). Bottles were shaken at 100 rpm at 37 °C. At designated time points, every 15 min for the first 2 h, 1 h for the next 8 h, and 3 h until the released drug concentration remained constant, 1 mL of the SBF release media was withdrawn and a UV−vis absorption spectrum of this sample was collected, using neat SBF as baseline absorption. The 1 mL of the SBF sample was then returned to the original SBF release media directly after the UV−vis measurement. The concentration of methylprednisolone species in the SBF release media was calculated by applying the Beer−Lambert law to its UV absorbance intensity at 248 nm, an adsorption wavelength associated with methylprednisolone species, using an extinction coefficient of 12 400 M^{-1} cm^{-1}. Exposure of surface-functionalized silica materials to an additional 100 mL of methylprednisolone-free simulated body fluid resulted in the release of more methylprednisolone, suggesting that its release from these materials may be limited by adsorption/desorption equilibrium under the conditions used.

Characterization. Small-angle X-ray diffraction (XRD) measurements enable characterization of mesoscopic ordering in SBA-15 derived silica materials and were obtained with a Philips XPERT MPD diffractometer using Cu Kα radiation.

The textural properties of the mesoporous silica materials were established by analysis of nitrogen adsorption−desorption isotherms at −196 °C obtained using a Micromeritics TRISTAR 3000 porosimiter. Prior to measurement, mesoporous SBA-15 silica materials were outgassed under vacuum at 300 °C, while materials with incorporated amino organosilica or C_{60} fullerene species were outgassed at 100 °C under vacuum. The adsorption−desorption isotherm measurements were performed according to the B.E.T. method using nitrogen adsorption points in the range P/P_0 = 0.05−0.2. Pore size distributions were determined by applying the Barret−Joyner−Halenda model (B.J.H.) to the adsorption branch of the

DOI: 10.1021/acs.jpcc.6b06238
J. Phys. Chem. C 2016, 120, 16887−16898

Table 1. Adsorption Properties, Zeta Potential Values at pH 7.4 and 4.6 and Methylprednisolone Loading Capacities of SBA-15 Silica Materials with and without Functionalities

	S_{BET} [a]		V_P [b]		D_p [c]	zeta potential		drug loading [d]
sample	$m^2\ g^{-1}$ material	$m^2\ g^{-1}$ silica	$cm^3\ g^{-1}$ material	$cm^3\ g^{-1}$ silica	(Å)	pH 7.4 (mV)	pH 4.6 (mV)	mg g^{-1} sample
SBA-15	582 ± 16	582 ± 16	0.78 ± 0.10	0.78 ± 0.10	82 ± 11	−15.9	−4.85	93
SBA-15-APS	391 ± 11	455 ± 13	0.73 ± 0.10	0.85 ± 0.11	82 ± 11	6.58	26.2	137
SBA-15-APS-$C_{60}H$	313 ± 9	376 ± 10	0.42 ± 0.06	0.50 ± 0.07	44 ± 6	−1.1	10.7	118
SBA-15-ABS	355 ± 10	409 ± 11	0.74 ± 0.11	0.85 ± 0.11	81 ± 11	9.59	26.3	117
SBA-15-ABS-$C_{60}H$	322 ± 9	400 ± 11	0.36 ± 0.05	0.44 ± 0.06	44 ± 6	−4.09	14.1	82
neat methylprednisolone						−23.0	−19.4	

[a]BET surface area. [b]Pore volume normalized to material or silica masses. [c]Modal pore size distribution. [d]Quantity of methylprednisolone sodium succinate loadings achieved by soaking materials in aqueous solutions containing methylprednisolone at concentrations of 50 mg mL^{-1}.

isotherm assuming a cylindrical pore geometry. For each sample, the average pore diameter was estimated as the value associated with the maximum intensity of the pore size distribution curve. Total pore volume was calculated at a relative pressure P/P_0 of 0.985.

NMR measurements conducted at Rey-Juan Carlos University, including one-dimensional (1D) solid-state $^{13}C\{^1H\}$ cross-polarization magic-angle-spinning (CP-MAS) and single-pulse ^{29}Si MAS NMR experiments, were performed on a Varian Infinity 400 MHz spectrometer fitted with a 9.4 T magnetic field. At this field strength, the ^{13}C and ^{29}Si nuclei Larmor frequencies are 100.53 and 79.41 MHz, respectively. Samples were packed in 7.5 mm zirconia rotors and experiments were conducted at room temperature under MAS conditions of 6 kHz using an H/X double-resonance 7.5 mm MAS probehead. For solid-state $^{13}C\{^1H\}$ CP-MAS experiments, the cross-polarization time was determined by the Hartmann−Hann[37] condition with 4.25 μs $\pi/2$ pulses, 2000 transients, a recycle delay of 3 s, and a CP contact time of 1 ms. ^{29}Si MAS single-pulse experiments had 3.5 μs $\pi/2$ pulse, 3000 transients, and recycle delay time of 60 s. ^{13}C and ^{29}Si chemical shifts were externally referenced to adamantane and tetramethylsilane, respectively.

Solid-state 1D and two-dimensional (2D) ^1H and ^{13}C NMR measurements were carried out on mesoporous SBA-15-APS-$C_{60}H$ silica samples without and with methylprednisolone guest species to understand intermolecular interactions among the guest species, organic surface moieties, and silica walls. Approximately 80 mg of sample was loaded into 4 mm zirconia MAS rotors for solid-state 1D and 2D NMR measurements. Solid-state 1D $^{13}C\{^1H\}$ CP measurements were conducted by a 4 mm double-resonance variable-temperature Bruker MAS probehead at 11.7 T using a Bruker AVANCE II spectrometer with operating frequencies of 500.24 MHz for ^1H and 125.79 MHz for ^{13}C. Cross-polarization was used to transfer magnetization from ^1H to ^{13}C nuclei by adiabatic passage according to the Hartmann−Hahn condition.[37] Solid-state 1D $^{13}C\{^1H\}$ CP measurements were conducted at room temperature under 12.5 kHz MAS conditions with a 2 ms CP contact time, recycle delay of 1 s, 10 000 transients, and with SPINAL-64 heteronuclear ^1H decoupling.[38]

Solid-state 2D $^{13}C\{^1H\}$ heteronuclear correlation (HETCOR) measurements were conducted using a 4 mm triple-resonance Bruker MAS probehead using a Bruker ASCEND-III NMR spectrometer at 9.4 T with operating frequencies of 400.02 MHz for ^1H and 100.64 MHz for ^{13}C. The 2D $^{13}C\{^1H\}$ HETCOR spectrum was acquired under 10 kHz MAS conditions, using a 2 ms CP contact time and 5 s recycle delay with 12 t_1 increments at an incremental size of 96 μs and 3072 transients each. Quadrature detection in the indirect (^1H) dimension was achieved using time-proportional phase-incrementation.[39] High power (100 kHz) $^1H-^1H$ homonuclear decoupling using the eDUMBO-1_{22} sequence was applied during the ^1H t_1 evolution period to enhance resolution in the ^1H dimension.[40] For the indirect dimension, a scaling factor of 0.60 was calibrated from a separate 2D $^{13}C\{^1H\}$ NMR spectrum of 99% ^{13}C- and ^{15}N-enriched glycine sample conducted under identical experimental conditions. During signal acquisition, heteronuclear ^1H decoupling was achieved using a SPINAL-64 pulse sequence[38] at a ^1H nutation frequency of 100 kHz. Separate 1D $^{13}C\{^1H\}$ CP-MAS and single-pulse ^1H spectra are shown at the top and alongside the 2D spectrum, respectively, and were acquired under identical experimental conditions as those of the associated 2D. Contour levels in the 2D spectra correspond to 5, 15, 25, 40, 55, and 75% of the maximum signal intensity. ^1H and ^{13}C chemical shifts in all 1D and 2D measurements were referenced to neat tetramethylsilane (TMS, 0 ppm), using tetrakismethylsilane as an external secondary reference (with ^{13}C and ^1H chemical shifts of 3.52 and 0.25 ppm relative to TMS, respectively).[41]

Amino organosilica and pharmaceutical guest loadings were determined by thermogravimetric analysis (TGA) with a Star System Mettler Thermobalance and, separately, elemental microanalyses with a Vario EL III apparatus. Zeta potentials were calculated based on measurements of the electrophoretic mobilities of bulk mesoporous materials using a zeta potential analyzer (Zetasizer Nano ZS, Iesmat).

RESULTS AND DISCUSSION

The quantities of aminopropyl organosilica species grafted to the silica surface of SBA-15-APS silica and adsorption properties of these materials are obtained from elemental analyses, TGA, solid-state NMR spectroscopy, and N_2 adsorption measurements. The carbon contents of SBA-15-APS materials can be directly related to the amounts of grafted organosilica species and establish aminopropyl organosilica loadings of 1.6 mmol per gram of SBA-15-APS material. Corroborative evidence for these organosilica loadings is provided by 1D single-pulse ^{29}Si NMR (Figure S1) and TGA (Figure S2) data, which indicate organosilica loadings of 1.0 and 1.1 mmol per gram of SBA-15-APS materials, respectively. Analyses of N_2 adsorption data reveal significantly reduced BET surfaces areas (Table 1) for SBA-15-APS (391 $m^2\ g^{-1}$ material) materials with respect to SBA-15 silica (582 $m^2\ g^{-1}$ material), which results, in part, from the added mass associated with grafted aminopropyl organosilica species. Normalizing the specific surface area to the mass of silica framework in SBA-

DOI: 10.1021/acs.jpcc.6b06238
J. Phys. Chem. C 2016, 120, 16887−16898

15-APS materials provides an adjusted surface area of 455 m^2 g^{-1} silica, reflecting that grafted aminopropyl organosilica species block mesopores and/or prevent N_2 adsorption to the silica surface.[17] However, pore blockage by incorporated organosilica species is unlikely, based on the highly similar pore volumes of SBA-15-APS materials (0.85 cm^3 g^{-1} silica) and mesoporous SBA-15 silica (0.78 cm^3 g^{-1} silica). These results establish that the surface areas of SBA-15-APS materials are similar to those of mesoporous SBA-15 silica materials, though are somewhat reduced by the presence of the grafted aminopropyl organosilica species. Interestingly, the average pore diameter of SBA-15-APS silica is nearly identical to that of mesoporous SBA-15 silica (Table 1). The high quantities of incorporated aminopropyl organosilica species, minimal pore blockage, and mesochannel pore sizes of SBA-15-APS materials are expected to enable incorporation of relatively high amounts of HC_{60} species.

The quantities of C_{60} incorporation and N_2 adsorption properties of SBA-15-APS-C_{60}H materials are established by elemental analysis, TGA, solid-state NMR spectroscopy, and N_2 adsorption. A comparison of the carbon contents of SBA-15-APS materials without and with HC_{60} species establishes C_{60} loadings of 0.17 mmol per gram of SBA-15-APS-C_{60}H material, which is in agreement with the 0.26 mmol C_{60} per gram obtained by analyses of TGA data (Table S1). Importantly, these incorporated C_{60} species appear to be covalently attached to aminopropyl organosilica species based on solid-state 1D $^{13}C\{^1H\}$ CP-MAS NMR spectra (Figure 1A) of SBA-15-APS-C_{60}H materials, which show a broad (full-width half-height of 10 ppm) ^{13}C signal at 135−155 ppm assignable to C_{60} moieties (Figure 1A, blue dot). A similarly broad ^{13}C NMR signal was attributed C_{60} species covalently bound to surface aminopropyl moieties in mesoporous MCM-41 silica, while sharp signals were observed for nonattached and mobile C_{60} species.[42] Therefore, the 1D NMR analysis provides strong evidence that C_{60} species incorporated into SBA-15-APS-C_{60}H materials are, in fact, attached to surface aminopropyl groups. Based on these results, approximately 31% of aminopropyl groups at the silica surface have covalently bound C_{60} functionalities, most of which likely reside at mesochannel surfaces nearby the silica particle surface because these regions are most accessible to solutions containing radical C_{60} species during the postsynthetic attachment process. Interestingly, despite the partial yield of HC_{60} attachment, incorporated HC_{60} groups considerably influence the N_2 adsorption properties of SBA-15-APS-C_{60}H materials. For example, SBA-15-APS-C_{60}H materials have dramatically reduced average pore diameters relative to SBA-15-APS materials (Table 1). The adjusted average pore volume (modified to account for incorporated organosilica and HC species) of SBA-15-APS-C_{60}H materials (0.50 cm^3 g^{-1} silica) is reduced compared to mesoporous SBA-15 materials (0.78 cm^3 g^{-1} silica), which could reflect either an excluded volume effect from incorporated C_{60} species or pore blockage by C_{60} species. The adjusted BET surface areas of SBA-15-APS-C_{60}H materials (376 m^2 g^{-1} silica support) are slightly lower than those of SBA-15-APS materials (433 m^2 g^{-1} silica support). The high hydrophobicities and surface areas of mesoporous silica functionalized with C_{60} species make these materials promising for the incorporation of large quantities of methylprednisolone species.

The methylprednisolone adsorption capacities of SBA-15, SBA-15-APS, and SBA-15-APS-C_{60}H materials are determined and shown to correlate qualitatively with the strengths of

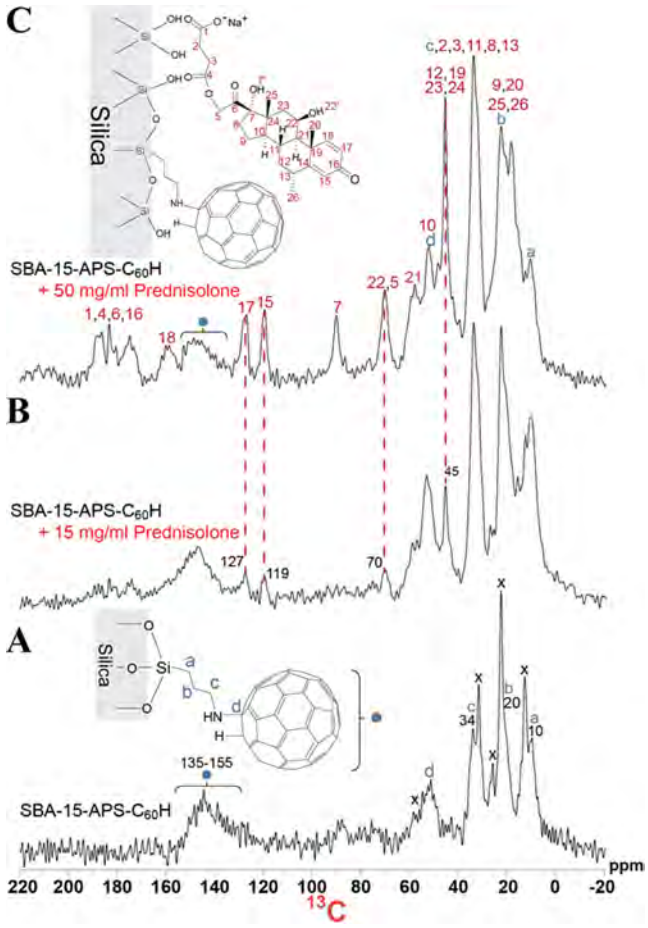

Figure 1. Solid-state 1D $^{13}C\{^1H\}$ CP-MAS spectra of mesoporous SBA-15 silica functionalized with HC_{60}-aminopropyl groups (A) without methylprednisolone, and with different loadings of methylprednisolone guest species achieved by exposing materials to solutions containing (B) 15 mg mL^{-1} and (C) 50 mg mL^{-1} methylprednisolone. The spectra were all acquired at room temperature under MAS conditions of 12.5 kHz with a 2 ms CP contact time ("X" indicates signals from THAB impurities).

electrostatic interactions between methylprednisolone and the silica surfaces. Adsorption of methylprednisolone species was achieved by exposing mesoporous SBA-15, SBA-15-APS and SBA-15-APS-C_{60}H materials to aqueous solutions containing methylprednisolone at concentrations of 50 mg mL^{-1}. Subsequent elemental analyses establish methylprednisolone loadings (Table 1) of 93 mg g^{-1} of mesoporous SBA-15 silica, and relatively greater loadings of 137 and 118 mg g^{-1} of SBA-15-APS and SBA-15-APS-C_{60}H materials, respectively. Differences in methylprednisolone loadings among these materials can be explained by the electrostatic interactions among the methylprednisolone and silica surfaces. As the zeta potential of pure methylprednisole sodium succinate is −23 mV (measured at pH 7.4), these species will have stronger attractive electrostatic interactions with, and greater adsorption to, silica surfaces having greater positive charge. As expected, SBA-15-APS materials have the most positive zeta potential (6.58 mV at pH 7.4, Table 1) and greatest methylprednisolone adsorption capacity, while mesoporous SBA-15 silicas with the most negative zeta potential (−15.9 mV at pH 7.4) exhibit the lowest capacities. These results demonstrate that attractive electrostatic interactions are important, though not solely responsible

DOI: 10.1021/acs.jpcc.6b06238
J. Phys. Chem. C 2016, 120, 16887−16898

for, methylprednisolone adsorption, as significant methylprednisolone adsorption is observed on surfaces that have negative surface charge and thus, on average, electrostatically repel methylprednisolone species (i.e., mesoporous SBA-15 silica). Therefore, attractive hydrogen-bonding and/or hydrophobic interactions also appear to influence methylprednisolone adsorption to silica surfaces.

Specific insights on intermolecular interactions between adsorbed methylprednisolone species and moieties at the functionalized mesoporous silica surfaces are provided by solid-state ^{13}C and ^{1}H NMR spectroscopy. For example, the solid-state 1D $^{13}C\{^{1}H\}$ CP-MAS NMR spectrum (Figure 1A) of SBA-15-APS-$C_{60}H$ materials without methylprednisolone reveals well-resolved ^{13}C signals associated with ^{13}C moieties of the HC_{60}-aminopropyl groups.[42] For example, the ^{13}C signals at 10, 20, 34, 52, and 135−155 ppm are assigned to ^{13}C moieties *a, b, c, d,* and those of the C_{60} fullerene (blue dot), respectively. Importantly, the $^{13}C\{^{1}H\}$ CP-MAS NMR spectrum (Figure 1B) of materials with low methylprednisolone loadings yields ^{13}C signals at 45, 70, 119, and 127 ppm (dotted red lines) that are not associated with ^{13}C moieties of the HC_{60}-aminopropyl groups (or THAB impurities). These signals, and others, correspondingly increase in intensity (Figure 1C) for materials with higher methylprednisolone loadings, and are confidently assigned to the ^{13}C moieties of the methylprednisolone species.[43] The ^{13}C signals associated with the alkyl moieties of the methylprednisolone guest have narrow line widths and reflect the relatively uniform ^{13}C molecular environments of these ^{13}C moieties for materials with both low and high methylprednisolone loadings, as shown in Figure 1B,C, respectively. A separate static (non-MAS) 1D $^{13}C\{^{1}H\}$ CP NMR spectrum of the sample with low methylprednisolone loading yields no resolved ^{13}C signals, which are broadened beyond detection (Figure S3). Hence, the narrow ^{13}C signals associated with the alkyl moieties of the methylprednisolone and HC_{60}-aminopropyl species can be concluded to result from relatively uniform MAS-averaged environments, rather than high molecular mobilities (relative to the 100 μs time scale of the NMR measurement). Interestingly, not all of the ^{13}C signals associated with the methylprednisolone species are narrow, in particular those at 170−190 ppm from the carboxylic or ketone groups (1, 4, 6, and 16) in Figure 1C. These results suggest that the adsorption of the methylprednisolone guests occurs via hydrogen-bonding of carboxylate moieties to surface silanol sites, as depicted in the schematic diagram in Figure 1C. Combined with analysis of zeta potential data, these results indicate that methylprednisolone species adsorb to the silica surface of SBA-15-APS-$C_{60}H$ materials based on electrostatic and hydrogen-bonding interactions.

While the solid-state 1D $^{13}C\{^{1}H\}$ CP-MAS NMR measurements yield molecular-level information about the HC_{60}-aminopropyl and methylprednisolone species, 2D $^{13}C\{^{1}H\}$ HETCOR measurements provide complementary insights on intermolecular interactions between these two species. Specifically, 2D $^{13}C\{^{1}H\}$ HETCOR measurements exploit through-space dipole−dipole couplings of locally proximate (<1 nm) ^{13}C and ^{1}H nuclei to correlate their isotropic chemical shifts. This provides direct information on intra- and intermolecular interactions among the chemically distinct ^{13}C and ^{1}H moieties of the HC_{60}-aminopropyl groups and methylprednisolone guests. In the 2D solid-state $^{13}C\{^{1}H\}$ HETCOR spectrum of Figure 2A, most of the observed intensity correlations are of intramolecular origin. These

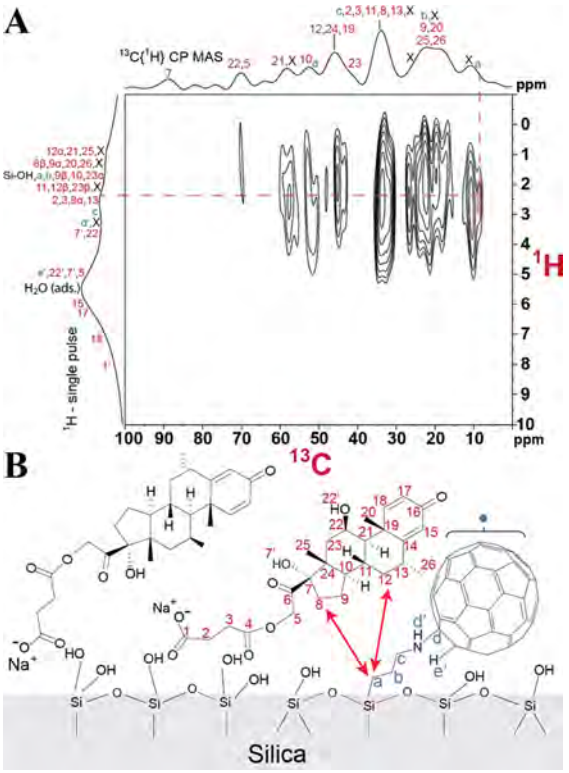

Figure 2. Solid-state 2D $^{13}C\{^{1}H\}$ dipolar-mediated HETCOR spectrum (A) of SBA-15-APS-$C_{60}H$ materials exposed to aqueous solutions containing 50 mg mL^{-1} methylprednisolone guest species. 1D $^{13}C\{^{1}H\}$ CP-MAS and single-pulse ^{1}H MAS spectra are shown along the top horizontal axis and the left vertical axis, respectively. The spectra were all acquired at room temperature under MAS conditions of 12.5 kHz with a 2 ms CP contact time. Schematic diagram (B) of methylprednisolone species at the HC_{60}-aminopropyl-functionalized silica surface with red and blue arrows that indicate intermolecular interactions consistent with the 2D NMR intensity correlations.

correlations corroborate the ^{13}C and ^{1}H signal assignments to specific moieties of the HC_{60}-aminopropyl group and methylprednisolone guests,[44−47] as labeled in the respective 1D single-pulse ^{1}H MAS and $^{13}C\{^{1}H\}$ CP-MAS spectra in Figure 2A.

Intensity correlations in the solid-state 2D $^{13}C\{^{1}H\}$ HETCOR spectrum in Figure 2 also arise from intermolecular interactions between HC_{60}-aminopropyl and methylprednisolone species and provide evidence for preferential association of the methylprednisolone guests with the aminopropyl, as opposed to the HC_{60}, moieties. Despite many of the overlapping ^{13}C signals of the HC_{60}-aminopropyl and methylprednisolone species, the ^{13}C signal associated with the *a* (8−9 ppm) methylene moieties of the HC_{60}-aminopropyl group are well-resolved. Importantly, correlated ^{13}C signals (8−9 ppm) associated with the *a* groups of the HC_{60}-aminopropyl moieties and ^{1}H signals (1.9−2.6 ppm, red shading) from the methylprednisolone alkyl moieties establishes the mutual interactions among HC_{60}-aminopropyl groups and methylprednisolone guests. Although intensity correlations associated with the ^{13}C signals of the alkyl moieties (<80 ppm) are observed, the 2D $^{13}C\{^{1}H\}$ HETCOR spectrum yields no correlated intensities in the ^{13}C region 140−148 ppm (not shown in Figure 2A) associated with the ^{13}C signals of the HC_{60} moieties. This may reflect relatively weak hydrophobic or $\pi-\pi$ interactions between methylprednisolone guests and the

DOI: 10.1021/acs.jpcc.6b06238
J. Phys. Chem. C 2016, 120, 16887−16898

HC_{60} moieties, or a relatively broad distribution of local interaction environments with the C_{60} fullerene. Due to the many overlapping ^{13}C signals of the HC_{60}-aminopropyl group and methylprednisolone guest in this 2D $^{13}C\{^1H\}$ HETCOR spectrum (Figure 2A) a specific configuration of the interacting methylprednisolone guest cannot be inferred and likely reflects a distribution of methylprednisolone configurations. Analysis of the 2D $^{13}C\{^1H\}$ HETCOR spectrum (Figure 2A) establishes the close (<1 nm) molecular proximities of HC_{60}-aminopropyl groups and methylprednisolone guests, providing direct evidence for intermolecular interactions among the aminopropyl groups and methylprednisolone alkyl moieties, as depicted in the schematic diagram in Figure 2B. We hypothesize that such interactions influence the release properties of methylprednisolone molecular guests.

The fractions and rates of methylprednisolone released from SBA-15, SBA-15-APS and SBA-15-APS-C_{60}H materials into simulated body fluids are quantified and analyzed to understand how surface aminopropyl and C_{60} moieties influence the release behaviors of methylprednisolone species. The amounts of methylprednisolone species released from mesoporous silica hosts into simulated body fluids under near neutral conditions (pH 7.4), corresponding to those in the bloodstream, can be estimated by using UV−visible spectroscopy to measure the absorbance intensity at 248 nm, which is associated with methylprednisolone molecules.[48] Specifically, the quantities of methylprednisolone released from mesoporous SBA-15, SBA-15-APS, or SBA-15-APS-C_{60}H silica materials were determined by applying the Beer−Lambert law to the absorbance intensities at 248 nm in UV−visible spectra acquired for simulated body fluids that were exposed for various time periods to these mesoporous silica host materials. Normalizing the amounts of released methylprednisolone species to the initial mass of methylprednisolone contained in the mesoporous SBA-15, SBA-15-APS, or SBA-15-APS-C_{60}H silica material yields the cumulative fractions of methylprednisolone released from these materials, as depicted in Figure 3A. After exposure to simulated body fluids, large fractions of the methylprednisolone species were released from all three of the mesoporous silica materials at times <500 min (Figure 3A). At times >500 min, the fractions of methylprednisolone released from these mesoporous hosts approach constant values that are lower than 100%, indicating incomplete extents of methylprednisolone release, due to diffusion resistances or sorption equilibrium of methylprednisolone species with the mesoporous silica surfaces. In particular, similar fractions of methylprednisolone (~80−90%) were released from mesoporous SBA-15, SBA-15-APS, and SBA-15-APS-C_{60}H silica materials, indicating that surface aminopropyl and C_{60} groups do not significantly influence the fractions of methylprednisolone released from functionalized mesoporous silica materials. However, methylprednisolone species were observed to release from the nonfunctionalized and functionalized mesoporous silica hosts at significantly different rates (Figure 3B), which were determined from the derivative of the cumulative methylprednisolone release profiles (Figure S5) at specific points in time. For example, higher rates of methylprednisolone release were observed for aminopropyl-functionalized SBA-15-APS materials, compared to nonfunctionalized mesoporous SBA-15 silica materials, which arise in part from the higher loadings of methylprednisolone in the former (137 mg g^{-1} material versus 93 mg g^{-1} material). More specifically, materials with higher methylprednisolone loadings are expected to have

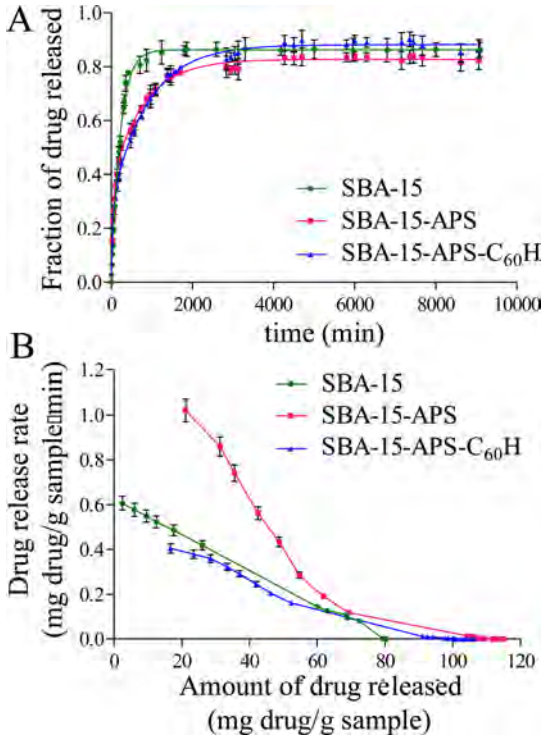

Figure 3. (A) Fractions of methylprednisolone released and (B) instantaneous release rates of methylprednisolone from nonfunctionalized mesoporous SBA-15 silica (green, circles), SBA-15-APS (pink, squares) and SBA-15-APS-C_{60}H (blue, triangles) materials into simulated body fluid (PBS buffer) at pH 7.4 and 37 °C. The instantaneous release rate values in (B) represent the derivative of a given cumulative release profile at a specific point in time, approximated by using a two-point finite difference formula.

larger release rates because of the increased prevalence of relatively weak drug−drug intermolecular interactions, versus stronger drug-host interactions, that facilitates methylprednisolone release into simulated body fluid. Additionally, the high loadings of methylprednisolone species yield large concentration gradients for the transport of methylprednisolone from the host to simulated body fluid, which likely contribute to the large release rates.[49] Importantly, Figure 3B also shows lower methylprednisolone release rates from SBA-15-APS-C_{60}H materials than from nonfunctionalized SBA-15 silica, despite the higher methylprednisolone loadings for the C_{60}-functionalized materials (118 mg g^{-1} material), compared to nonfunctionalized mesoporous SBA-15 silica (93 mg g^{-1} material). These results establish that the release of methylprednisolone species from mesoporous silica materials is mediated by surface-grafted C_{60} moieties, presumably due to steric effects[31] that are also evidenced by the significantly reduced pore diameters (Table 1) for SBA-15-APS-C_{60}H materials relative to SBA-15 and SBA-15-APS silica materials. The high hydrophobicities of C_{60} species may also inhibit the influx of aqueous simulated body fluids into mesoporous SBA-15-APS-C_{60}H materials, thereby reducing methylprednisolone transport within the mesochannels.

The methylprednisolone release from the aminopropyl-functionalized mesoporous SBA-15-APS and SBA-15-APS-C_{60}H silica materials into simulated body fluids can be described by using first-order and Korsmeyer-Peppas[50] kinetic models. The first-order kinetic model for drug release assumes that the rate of methylprednisolone release from a mesoporous

DOI: 10.1021/acs.jpcc.6b06238
J. Phys. Chem. C 2016, 120, 16887−16898

silica host material is proportional to the concentration of pharmaceuticals in the simulated body fluid. Smaller first-order rate coefficients (the constants of proportionality) correspond to lower release rates of methylprednisolone from the mesoporous silica hosts. Analyses of the cumulative methylprednisolone release profiles (Figure S5) using the first-order kinetic model reveal that the lowest first-order rate coefficients (0.0072 min^{-1}) are associated with the SBA-15-APS-C_{60}H materials, compared to nonfunctionalized mesoporous SBA-15 (0.0080 min^{-1}) and SBA-15-APS silica (0.0201 min^{-1}). These relative values are consistent with mediated transport of methylprednisolone within the mesochannels by C_{60} moieties grafted to the silica surface. By comparison, the Korsmeyer–Peppas kinetic model for drug release provides complementary insight about the diffusion of methylprednisolone molecules within mesoporous silica materials, in particular whether diffusion occurs by Fickian or non-Fickian processes. Cumulative methylprednisolone release profiles associated with SBA-15-APS and SBA-15-APS-C_{60}H materials are fitted well by the Korsmeyer-Peppas model, according to the R^2 values listed in Table S2. Assuming spherical particle geometries for the SBA-15-APS and SBA-15-APS-C_{60}H materials, the Korsmeyer-Peppas fitting analyses suggest non-Fickian diffusion for methylprednisolone molecules within these functionalized mesoporous materials, within the standard errors associated with the analyses. Such diffusion processes are consistent with the impeded diffusion of methylprednisolone within functionalized mesoporous materials by the nanoscale pore dimensions and/or the interactions among methylprednisolone and moieties at the silica surfaces.

As functionalities at the silica surface of mesoporous silicas can significantly influence methylprednisolone adsorption and release behaviors, materials grafted with either aminobutyl organosilica species were evaluated as hosts for methylprednisolone delivery. The amounts of aminobutyl and aminobutyl-C_{60} organosilica species grafted to SBA-15-ABS and SBA-15-ABS-C_{60}H materials, respectively, were similar to those for SBA-15 materials functionalized with aminopropyl organosilica species. The adsorption and release behaviors of methylprednisolone in aminobutyl-functionalized SBA-15-ABS and SBA-15-ABS-C_{60}H materials into simulated body fluid (pH 7.4) were quantified and can be explained by the intermolecular interactions among methylprednisolone and moieties at the functionalized mesoporous silica surfaces. The capacities for methylprednisolone adsorption were lower for SBA-15-ABS-C_{60}H materials (82 mg g^{-1} sample), than for SBA-15-ABS materials (117 mg g^{-1} sample), which are consistent with stronger attractive electrostatic interactions between methylprednisolone and the silica surfaces of SBA-15-ABS materials as established by the zeta potential values (Table 1) of the respective materials. Exposure of methylprednisolone-loaded mesoporous SBA-15-ABS or SBA-15-ABS-C_{60}H silica materials to simulated body fluids resulted in the incomplete release of methylprednisolone species, again likely due to diffusion limitations or sorption equilibrium of methylprednisolone with the functionalized silica surfaces. Interestingly, approximately 90% of methylprednisolone was released from nonfunctionalized mesoporous SBA-15 silica materials, while lower fractions of 75% and 50% were released from mesoporous SBA-15-ABS and SBA-15-ABS-C_{60}H silica materials, respectively. The instantaneous rates of methylprednisolone release (Figure 4B) from the mesoporous SBA-15-ABS and SBA-15-ABS-C_{60}H silica materials were lower than from

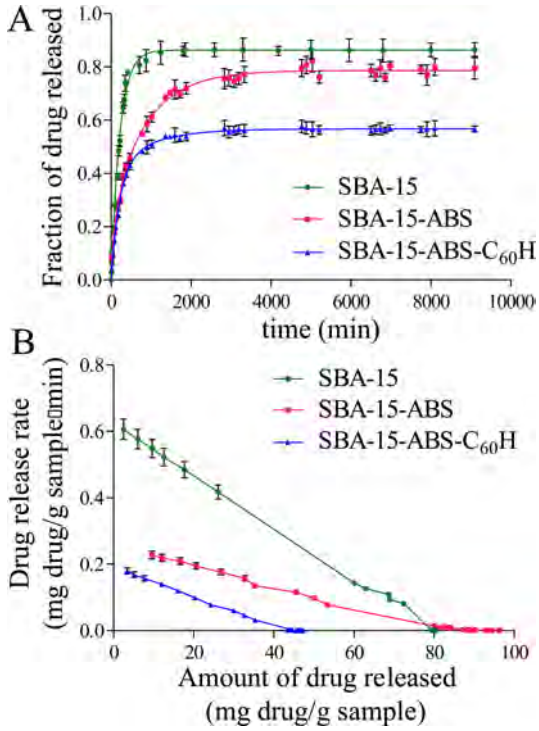

Figure 4. (A) Fractions of methylprednisolone released and (B) instantaneous release rates of methylprednisolone from nonfunctionalized mesoporous SBA-15 silica (green, circles), SBA-15-ABS (pink, squares), and SBA-15-ABS-C_{60}H (blue, triangles) materials into simulated body fluid (PBS buffer) at pH 7.4 and 37 °C. The instantaneous release rate values in (B) represent the derivative of a given cumulative release profile at a specific point in time, approximated by using a two-point finite difference formula.

nonfunctionalized mesoporous SBA-15 silica, despite the greater loadings of methylprednisolone for the functionalized mesoporous silica materials. These results establish that the release of methylprednisolone species from the mesoporous SBA-15-ABS and SBA-15-ABS-C_{60}H silica materials can be mediated by the grafted aminobutyl and C_{60} moieties at the mesoporous surface. Moreover, analyses of the instantaneous release profiles (Figure S3) of SBA-15-ABS and SBA-15-ABS-C_{60}H materials using a first-order kinetic release model yields first-order rate coefficients of 0.0034 and 0.0045 min^{-1}, respectively. These rate coefficients are lower than those associated with nonfunctionalized mesoporous SBA-15 silica (0.0080 min^{-1}), establishing the slower release of methylprednisolone from the mesoporous silica materials with aminobutyl and/or C_{60} surface functionalities. Using the Korsmeyer-Peppas kinetic model as previously described indicates that methylprednisolone molecules diffuse by a non-Fickian process in SBA-15-ABS and SBA-15-ABS-C_{60}H materials, just as in the case of aminopropyl functionalized mesoporous silica.

Notable differences in the release behaviors of methylprednisolone species from aminopropyl-functionalized SBA-15-APS-C_{60}H and aminobutyl-functionalized SBA-15-ABS-C_{60}H materials into simulated body fluids (pH 7.4) are observed despite the similar quantities of grafted amino organosilica and HC_{60} species in these two materials. For example, the fractions of methylprednisolone released from SBA-15-APS-C_{60}H and SBA-15-ABS-C_{60}H materials were 90% and 50%, respectively, as shown in Figure 5A. The relatively low fractions of

DOI: 10.1021/acs.jpcc.6b06238
J. Phys. Chem. C 2016, 120, 16887−16898

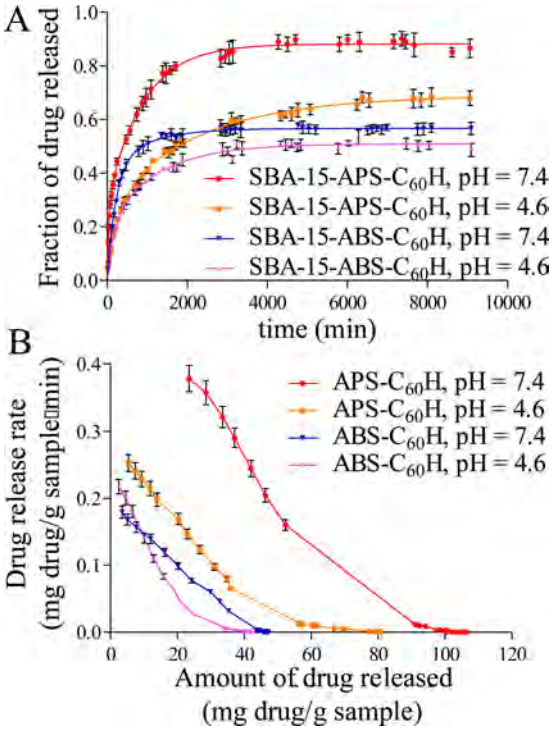

Figure 5. (A) Fractions of methylprednisolone released and (B) instantaneous release rates of methylprednisolone from SBA-15-APS-C_{60}H into simulated body fluids at pH 7.4 (red, circles) and pH 4.6 (orange, squares), and from SBA-15-ABS-C_{60}H into simulated body fluids at pH 7.4 (blue, triangles) and pH 4.6 (pink, stars). The simulated body fluids at pH 4.6 were acetate buffered solutions, while those at pH 7.4 were PBS buffered solutions, and all release experiments were conducted at 37 °C. The instantaneous release rate values in (B) represent the derivative of a given cumulative release profile at a specific point in time, approximated by using a two-point finite difference formula.

methylprednisolone released from mesoporous SBA-15-ABS-C_{60}H silica materials correlate with the lower methylprednisolone loadings in SBA-15-ABS-C_{60}H materials (82 mg g^{-1} material), compared to SBA-15-APS-C_{60}H materials (118 mg g^{-1} material), and may be influenced also by stronger interactions of methylprednisolone species with the more hydrophobic aminobutyl versus aminopropyl surface moieties. Additionally, as shown in Figure 5B, lower rates of methylprednisolone release were observed from mesoporous SBA-15-ABS-C_{60}H, compared to SBA-15-APS-C_{60}H silica materials, which reflects in part the greater methylprednisolone loadings in SBA-15-APS-C_{60}H materials. However, analyses of the cumulative profiles of methylprednisolone release (Figure S3) for the C_{60}-functionalized mesoporous materials using a first-order kinetic release model yields lower first-order rate coefficients associated with the SBA-15-ABS-C_{60}H materials (0.0045 min^{-1}) than for the SBA-15-APS-C_{60}H materials (0.0072 min^{-1}), as shown in Table S2.

The slower release of methylprednisolone from mesoporous silicas that have aminobutyl-C_{60}H, versus aminopropyl-C_{60}H, surface moieties may be due to differences in their respective steric, hydrogen-bonding or electrostatic interactions, or methylprednisolone loadings. Based on the modestly different lengths of the alkyl chains of aminopropyl and aminobutyl surface moieties, it is expected that SBA-15-APS-C_{60}H and SBA-15-ABS-C_{60}H materials will result in similar steric impediments to methylprednisolone diffusion within mesopores; such similarities are consistent with the identical mean BET pore diameters (4.4 ± 0.6 nm, Table 1) of both materials and with recent molecular simulations and analyses by Doadrio et al. on the release of dye species from similarly functionalized mesoporous silicas.[51] Both C_{60}-functionalized materials also have similar quantities of aminoalkyl surface functionalities and so are expected to exhibit similar extents of hydrogen-bonding interactions with methylprednisolone species. By comparison, the lower zeta potential values (Table 1) associated with SBA-15-ABS-C_{60}H, compared to SBA-15-APS-C_{60}H, materials indicate that the former manifest weaker electrostatic interactions with methylprednisolone guests. However, if predominant, such weaker interactions would be expected to lead to faster rates of release for SBA-15-ABS-C_{60}H materials, which is opposite to what is observed for the macroscopic release data. The lower release rates observed for SBA-15-ABS-C_{60}H materials are consistent with the relatively lower methylprednisolone loadings of SBA-15-ABS-C_{60}H (82 mg drug/sample) versus those of SBA-15-APS-C_{60}H (118 mg drug/g sample) materials, which impart smaller concentration gradients to drive diffusion and release from the host materials.

Exposure of C_{60}-functionalized mesoporous silica materials to simulated body fluids under acidic conditions (pH 4.6), corresponding to those nearby tumors, yields lower fractions and rates of methylprednisolone release compared to under near neutral conditions (pH 7.4). For example, while approximately 85% of the total methylprednisolone species were released from SBA-15-APS-C_{60}H materials under near neutral conditions, lower fractions of ~70% were released from identical materials under acidic conditions, as shown in Figure 5A. Similarly reduced fractions of methylprednisolone were released from SBA-15-ABS-C_{60}H materials under acidic conditions. The lower fractions of methylprednisolone released from these C_{60}-functionalized silica materials are consistent with the increased attractive electrostatic interactions among methylprednisolone and the functionalized silica surfaces under acidic versus near neutral conditions, as evidenced by the zeta potential measurements (Table 1) of the corresponding materials. Similarly, the reduced rates of methylprednisolone release from SBA-15-APS-C_{60}H and SBA-15-ABS-C_{60}H materials under acidic conditions, as shown in Figure 5B, are also consistent with the increased attractive electrostatic interactions. Analyses of methylprednisolone release profiles into acidic simulated body (Figure S5C) using the Korsmeyer-Peppas kinetic model reveal similar non-Fickian diffusion processes for methylprednisolone in both SBA-15-APS-C_{60}H and SBA-15-ABS-C_{60}H materials, as observed under near neutral conditions. The reduced rates of methylprednisolone release from C_{60}-functionalized materials under acidic conditions would promote longer durations of pharmaceutical release from these materials in the vicinity of tumors. Therefore, if used for tumor treatment, the C_{60}-functionalized materials could allow the pharmaceutical to be administered less frequently to patients, which could subsequently improve patient compliance.

CONCLUSIONS

The molecular-level interactions among a representative pharmaceutical species, methylprednisolone sodium succinate, and moieties on the interior surfaces of mesoporous SBA-15 silica materials were established and correlated with bulk adsorption properties. Specifically, mesoporous SBA-15 silica

DOI: 10.1021/acs.jpcc.6b06238
J. Phys. Chem. C 2016, 120, 16887−16898

materials with aminopropyl or aminobutyl surface moieties without and with C_{60} species were characterized and evaluated for the adsorption of methylprednisolone species. Methylprednisolone adsorption to these materials was shown to depend strongly on the electrostatic interactions among methylprednisolone molecules and the functionalized silica surfaces, which correlate with the different loadings for the functionalized materials. Complementary solid-state 1D $^{13}C\{^1H\}$ CP-MAS NMR measurements provided evidence for hydrogen-bonding between methylprednisolone species and the silica surface, while 2D $^{13}C\{^1H\}$ HETCOR NMR techniques established the close molecular proximities of the alkyl moieties of methylprednisolone species and aminopropyl functionalities at the silica surface, suggesting attractive hydrophobic interactions among these species. These results indicate that the adsorption of methylprednisolone to SBA-15 materials functionalized with HC_{60}-amino organosilica species involves contributions from electrostatic, hydrogen-bonding, and hydrophobic interactions.

The transient release of methylprednisolone from functionalized mesoporous SBA-15 silica materials into simulated body fluids was monitored to understand the influence of the different surface functionalities on methylprednisolone release behaviors. The surface-grafted aminopropyl, aminobutyl, and C_{60} surface moieties of functionalized mesoporous silica materials appear to reduce the rates of methylprednisolone release by a combination of electrostatic, hydrophobic and steric effects. Indeed, C_{60}-functionalized SBA-15-APS-C_{60}H and SBA-15-ABS-C_{60}H materials showed the slowest methylprednisolone release rates of all materials investigated. Methylprednisolone release from these functionalized mesoporous silica materials was evaluated under acidic and near neutral pH conditions, which correspond to conditions nearby tumors and in the bloodstream, respectively. Lower fractions and rates of methylprednisolone release were observed from C_{60}-functionalized mesoporous silica materials under acidic conditions (pH 4.6) versus near neutral conditions (pH 7.4), which were attributed to stronger electrostatic interactions among methylprednisolone and the surfaces of the C_{60}-functionalized SBA-15 silica. These results demonstrate that the types of surface-grafted alkylamino and C_{60} functionalities can mediate pharmaceutical release from functionalized mesoporous silica materials. The detailed understanding of molecular-level properties and interactions of methylprednisolone and C_{60}-functionalized mesoporous silicas developed here provides important information for designing effective silica-based drug-delivery systems.

■ ASSOCIATED CONTENT

Supporting Information

The Supporting Information is available free of charge on the ACS Publications website at DOI: 10.1021/acs.jpcc.6b06238.

Quantities of amino organosilica and C_{60} fullerene species incorporated into mesoporous SBA-15 silica materials, kinetic parameters values, solid-state ^{29}Si MAS NMR spectra, solid-state 1D ^{13}C CP-MAS NMR spectra, solid-state 1D $^{13}C\{^1H\}$ CP-MAS NMR spectra, thermogravimetric analyses plots, and the cumulative profiles of methylprednisolone released. (PDF)

■ AUTHOR INFORMATION

Corresponding Authors

*E-mail: rafael.garcia@urjc.es. Phone: +34 91 4887086. Fax: +34 91 4887068.

*E-mail: bradc@engineering.ucsb.edu.

Notes

The authors declare no competing financial interest.

■ ACKNOWLEDGMENTS

The work at Rey Juan Carlos University was supported by the Spanish government projects CTQ2014-57858-R and CTQ2011-22707. The work at UCSB was supported in part by the Institute for Collaborative Biotechnologies through Grant W911NF-09-D-0001 from the U.S. Army Research Office. The NMR experiments were conducted using the Central Facilities of the UCSB Materials Research Laboratory supported by the MRSEC program of the U.S. NSF under Award No. DMR-1121053.

■ REFERENCES

(1) Wang, S. Ordered mesoporous materials for drug delivery. *Microporous Mesoporous Mater.* **2009**, *117*, 1−9.

(2) Slowing, I. I.; Vivero-Escoto, J. L.; Wu, C. W.; Lin, V. S. Y. Mesoporous silica nanoparticles as controlled release drug delivery and gene transfection carriers. *Adv. Drug Delivery Rev.* **2008**, *60*, 1278−1288.

(3) Calvillo, L.; Celorrio, V.; Moliner, R.; Cabot, P. L.; Esparbé, I.; Lázaro, M. J. Control of textural properties of ordered mesoporous materials. *Microporous Mesoporous Mater.* **2008**, *116*, 292−298.

(4) Izquierdo-Barba, I.; Sousa, E.; Doadrio, J. C.; Doadrio, A. L.; Pérez-Pariente, J.; Martínez, A.; Babonneau, F.; Vallet-Regí, M. Influence of mesoporous structure type on the controlled delivery of drugs: release of ibuprofen from MCM-48, SBA-15 and functionalized SBA-15. *J. Sol-Gel Sci. Technol.* **2009**, *50*, 421−429.

(5) Gignone, A.; Delle Piane, M.; Corno, M.; Ugliengo, P.; Onida, B. Simulation and Experiment Reveal a Complex Scenario for the Adsorption of an Antifungal Drug in Ordered Mesoporous Silica. *J. Phys. Chem. C* **2015**, *119* (23), 13068−13079.

(6) Lei, C.; Shin, Y.; Liu, J.; Ackerman, E. J. Entrapping enzyme in a functionalized nanoporous support. *J. Am. Chem. Soc.* **2002**, *124*, 11242−11243.

(7) Maria-Chong, A. S.; Zhao, X. S. Functionalization of SBA-15 with APTES and characterization of functionalized materials. *J. Phys. Chem. B* **2003**, *107*, 12650−12657.

(8) Liu, Y. H.; Lin, H. P.; Mou, C. Y. Direct method for surface silyl functionalization of mesoporous silica. *Langmuir* **2004**, *20*, 3231−3239.

(9) Shimojima, A.; Umeda, N.; Kuroda, K. Synthesis of layered inorganic-organic nanocomposite films from mono-, di-, and trimethoxy(alkyl)silanetetramethoxysilane systems. *Chem. Mater.* **2001**, *13*, 3610−3616.

(10) Jia, M.; Seifert, A.; Thiel, W. R. Mesoporous MCM-41 materials modified with oxodiperoxo molybdenum complexes: efficient catalysts for the epoxidation of cyclooctene. *Chem. Mater.* **2003**, *15*, 2174−2180.

(11) Hoffmann, F.; Cornelius, M.; Morell, J.; Fröba, M. Silica-based mesoporous organic-inorganic hybrid materials. *Angew. Chem., Int. Ed.* **2006**, *45*, 3216−3251.

(12) Lin, V. S. Y.; Lai, C. Y.; Huang, J.; Song, S. A.; Xu, S. Molecular recognition inside of multifunctionalized mesoporous silicas: Toward selective fluorescence detection of dopamine and glucosamine. *J. Am. Chem. Soc.* **2001**, *123*, 11510−11511.

(13) Mal, N. K.; Fujiwara, M.; Tanaka, Y.; Taguchi, T.; Matsukata, M. Photo-switched storage and release of guest molecules in the pore void of coumarin-modified MCM-41. *Chem. Mater.* **2003**, *15*, 3385−3394.

DOI: 10.1021/acs.jpcc.6b06238
J. Phys. Chem. C 2016, 120, 16887−16898

(14) Mal, N. K.; Fujiwara, M.; Tanaka, Y. Photocontrolled reversible release of guest molecules from coumarin-modified mesoporous silica. *Nature* **2003**, *421*, 350−353.
(15) García, N.; Benito, E.; Guzmán, J.; Tiemblo, P.; Morales, V.; García, R. A. Functionalization of SBA-15 by an acid-catalyzed approach. A surface characterization study. *Microporous Mesoporous Mater.* **2007**, *106*, 129−139.
(16) Matsumoto, A.; Tsutsumi, K.; Schumacher, J.; Unger, K. K. Surface functionalization and stabilization of mesoporous silica spheres by silanization and their adsorption characteristics. *Langmuir* **2002**, *18*, 4014−4019.
(17) Anwander, R.; Nagl, I.; Widenmeyer, M.; Engelhardt, G.; Groeger, O.; Plam, C.; Röser, T. Surface characterization and functionalization of MCM-41 silicas via silazane silylation. *J. Phys. Chem. B* **2000**, *104*, 3532−3544.
(18) Inumura, K.; Inoue, Y.; Kakii, S.; Nakano, T.; Yamanaka, S. Molecular selective adsorption of dilute alkylphenols and alkylanilines from water by alkyl-grafted MCM-41: tunability of the cooperative organic−inorganic function in the nanostructure. *Phys. Chem. Chem. Phys.* **2004**, *6*, 3133−3139.
(19) Martin, T.; Galarneau, A.; Di Renzo, F.; Brunel, D.; Fajula, F.; Heinisch, S.; Crétier, G.; Rocca, J. L. Great improvement of chromatographic performance using MCM-41 spheres as stationary phase in HPLC. *Chem. Mater.* **2004**, *16*, 1725−1731.
(20) Song, S.-W.; Hidajat, K.; Kawi, S. Functionalized SBA-15 materials as carriers for controlled drug delivery: Influence of surface properties on matrix-drug interactions. *Langmuir* **2005**, *21*, 9568−9575.
(21) Trens, P.; Russell, M. L.; Spjuth, L.; Hudson, M. J.; Liljenzin, J. O. Preparation of malonamide-MCM-41 materials for the heterogeneous extraction of radionuclides. *Ind. Eng. Chem. Res.* **2002**, *41*, 5220−5225.
(22) Rodríguez-López, G.; Marcos, M. D.; Martínez-Máñez, R.; Sancenón, F.; Soto, J.; Villaescusa, L. A.; Beltrán, D.; Amorós, P. Efficient boron removal by using mesoporous matrices grafted with saccharides. *Chem. Commun.* **2004**, *19*, 2198−2199.
(23) Tourné-Péteilh, C.; Brunel, D.; Bégu, S.; Chiche, B.; Fajula, F.; Lerner, D. A.; Devoisselle, J. M. Synthesis and characterization of ibuprofen-anchored MCM-41 silica and silica gel. *New J. Chem.* **2003**, *27*, 1415−1418.
(24) Martín, A.; García, R. A.; Sen Karaman, D.; Rosenholm, J. M. Polyethyleneimine-functionalized large pore ordered silica materials for poorly water-soluble drug delivery. *J. Mater. Sci.* **2014**, *49*, 1437−1447.
(25) Doadrio, J. C.; Sousa, E. M. B.; Izquierdo-Barba, I.; Doadrio, A. L.; Pérez-Pariente, J.; Vallet-Regí, M. Functionalization of mesoporous materials with long alkyl chains as a strategy for controlling drug delivery pattern. *J. Mater. Chem.* **2006**, *16*, 462−467.
(26) Qu, F.; Zhu, G.; Huang, S.; Li, S.; Qiu, S. Effective controlled release of captopril by silylation of mesoporous MCM-41. *ChemPhysChem* **2006**, *7*, 400−406.
(27) Tang, Q.; Xu, Y.; Wu, D.; Sun, Y. Hydrophobicity-controlled drug delivery system from organic modified mesoporous silica. *Chem. Lett.* **2006**, *35*, 474−475.
(28) Diao, X.; Wang, Y.; Zhao, J.; Zhu, S. Effect of pore size of mesoporous SBA-15 on adsorption of bovine serum albumin and lysozyme protein. *Chin. J. Chem. Eng.* **2010**, *18*, 493−499.
(29) Doadrio, A. L.; Salinas, A. J.; Sánchez-Montero, J. M.; Vallet-Regí, M. Drug Release from Ordered Mesoporous Silicas. *Curr. Pharm. Des.* **2015**, *21*, 6213.
(30) Lee, C.; Lin, T.; Lin, H.; Zhao, Q.; Liu, S.; Mou, C. High loading of C_{60} into nanochannels of mesoporous MCM-41 materials. *Microporous Mesoporous Mater.* **2003**, *57*, 199−209.
(31) García-Muñoz, R. A.; Morales, V.; Linares, M.; González, P. E.; Sanz, R.; Serrano, D. P. Influence of the structural and textural properties of ordered mesoporous materials and hierarchical zeolitic supports on the controlled release of methylprednisolone hemisuccinate. *J. Mater. Chem. B* **2014**, *2*, 7996−8004.
(32) Zhao, D.; Feng, J.; Huo, Q.; Melosh, N.; Frederickson, G. H.; Chmelka, B. F.; Stucky, G. D. Triblock copolymer syntheses of mesoporous silica with periodic 50 to 300 angstrom pores. *Science* **1998**, *279*, 548−622.
(33) Nakamura, E.; Isobe, H.; Tomita, H.; Sawamura, M.; Jinno, S.; Okayama, H. Functionalized fullerene as an artificial vector for transfection. *Angew. Chem., Int. Ed.* **2000**, *39*, 4254−4257.
(34) Uritu, C. M.; Varganici, C. D.; Ursu, L.; Coroaba, A.; Nicolescu, A.; Dascalu, A. I.; Peptanariu, D.; Stan, D.; Constantinescu, C. A.; Simion, V.; et al. Hybrid fullerene conjugates as vectors for DNA cell-delivery. *J. Mater. Chem. B* **2015**, *3*, 2433−2446.
(35) Yamago, S.; Tokuyama, H.; Nakamuralr, E.; Kikuchi, K.; Kananishl, S.; Sueki, K.; Nakahara, H.; Enomoto, S.; Ambe, F. In vivo biological behavior of a water-miscible fullerene: ^{14}C labeling, absorption, distribution, excretion and acute toxicity. *Chem. Biol.* **1995**, *2*, 385−389.
(36) Lankoff, A.; Arabski, M.; Wegierek-Ciuk, A.; Kruszewski, M.; Lisowska, H.; Banasik-Nowak, A.; Rozga-Wijas, K.; Wojewodzka, M.; Slomkowski, S. Effect of surface modification of silica nanoparticles on toxicity and cellular uptake by human peripheral blood lymphocytes in vitro. *Nanotoxicology* **2012**, *7*, 235−250.
(37) Hediger, S.; Meier, B. H.; Kurur, N. D.; Bodenhausen, G.; Ernst, R. R. NMR cross-polarization by adiabatic passage through the Hartmann-Hahn condition (APHH). *Chem. Phys. Lett.* **1994**, *223*, 283−288.
(38) Fung, B. M.; Khitrin, A. K.; Ermolaev, K. An improved broadband decoupling sequence for liquid crystals and solids. *J. Magn. Reson.* **2000**, *142*, 97−101.
(39) Marion, D.; Wüthrich, K. Application of phase sensitive two-dimensional correlated spectroscopy (COSY) for measurements of ^{1}H-^{1}H spin-spin coupling constants in proteins. *Biochem. Biophys. Res. Commun.* **1983**, *113*, 967−974.
(40) Elena, B.; de Paëpe, G.; Emsley, L. Direct spectral optimization of proton-proton homonuclear decoupling in solid-state NMR. *Chem. Phys. Lett.* **2004**, *398*, 532−538.
(41) Hayashi, S.; Hayamizu, K. Chemical shift standards in high-resolution solid-state NMR (1) ^{13}C, ^{29}Si, and ^{1}H nuclei. *Bull. Chem. Soc. Jpn.* **1991**, *64*, 685−687.
(42) Lee, C.; Lin, T.; Lin, H.; Zhao, Q.; Liu, S.; Mou, C. High loading of C_{60} into nanochannels of mesoporous MCM-41 materials. *Microporous Mesoporous Mater.* **2003**, *57*, 199−209.
(43) Valliant, J. F.; Schaffer, P.; Britten, J. F.; Davidson, A.; Jones, A. G.; Yanch, J. C. The synthesis of corticosteroid-carborane esters for the treatment of rheumatoid arthritis via boron neutron capture synovectomy. *Tetrahedron Lett.* **2000**, *41*, 1355−1358.
(44) Cheng, J.; Xenopoulos, A.; Wunderlich, B. Two-dimensional NMR studies on the additivity rules for carbon-1 chemical 3 shifts in tetra-n-alkylammonium halides. *Magn. Reson. Chem.* **1992**, *30*, 917−926.
(45) Zhang, Z. G.; Li, H.; Qi, B.; Chi, D.; Jin, Z.; Qi, Z.; Hou, J.; Li, Y.; Wang, J. Amine group functionalized fullerene derivatives as cathode buffer layers for high performance polymer solar cells. *J. Mater. Chem. A* **2013**, *1*, 9624−9629.
(46) Dzhemilev, U. M.; Ibrahimov, A. G.; Tuktarov, A. R.; D'yakonov, V. A.; Pudas, M.; Bergmann, U. Catalytic hydroamination of fullerene C_{60} with primary and secondary amines. *Russ. J. Org. Chem.* **2007**, *43*, 375−379.
(47) Spielmann, H. P.; Wang, G. W.; Meier, M. S.; Weedon, B. R. Preparation of $C_{70}H_2$, $C_{70}H_4$, and $C_{70}H_8$: Three independent reduction manifolds in the Zn(Cu) reduction of C_{70}. *J. Org. Chem.* **1998**, *63*, 9865−9871.
(48) Vree, T. B.; Lagerwerf, A. J.; Verwey-van Wissen, C. P. W. G. M.; Jongen, P. J. H. High-performance liquid chromatography analysis, preliminary pharmacokinetics, metabolism and renal excretion of methylprednisolone with its C6 and C20 hydroxy metabolites in multiple sclerosis patients receiving high-dose pulse therapy. *J. Chromatogr., Biomed. Appl.* **1999**, *732* (2), 337−348.
(49) Vallet-Regí, M.; Izquierdo-Barba, I.; Colilla, M. Structure and functionalization of mesoporous bioceramics for bone tissue

DOI: 10.1021/acs.jpcc.6b06238
J. Phys. Chem. C 2016, 120, 16887−16898

regeneration and local drug delivery. *Philos. Trans. R. Soc., A* **2012**, *370*, 1400−1421.
(50) Korsmeyer, R. W.; Gurny, R.; Doelker, E.; Buri, P.; Peppas, N. A. Mechanism of potassium chloride release from compressed, hydrophilic, polymeric matrices: effect of entrapped air. *J. Pharm. Sci.* **1983**, *72* (10), 1189−1191.
(51) Doadrio, A. L.; Sánchez-Montero, J. M.; Doadrio, J. C.; Salinas, A. J.; Vallet-Regí, M. A molecular model to explain the controlle d release from SBA-15 functionalized with APTES. *Microporous Mesoporous Mater.* **2014**, *195*, 43−49.

DOI: 10.1021/acs.jpcc.6b06238
J. Phys. Chem. C 2016, 120, 16887−16898

Correlating Surface-Functionalization of Mesoporous Silica with Adsorption and Release of Pharmaceutical Guest Species

Victoria Morales,[1] Matthew N. Idso,[2] Moisés Balabasquer,[1] Bradley Chmelka,[2] Rafael A. García-Muñoz[1*]*

[1]Group of Chemical and Environmental Engineering, ESCET, Rey Juan Carlos University. C/ Tulipán s/n, E-28933 Móstoles, Madrid, Spain.

[2]Department of Chemical Engineering, University of California, Santa Barbara, California 93106 U.S.A.

SUPPORTING INFORMATION

Table S1. Quantities of amino organosilica and C_{60} fullerene species incorporated into mesoporous SBA-15 silica materials calculated from mass percent C as determined by elemental analysis, thermogravimetric analysis (TGA) and solid-state ^{29}Si single-pulse MAS NMR measurements.

Sample	mmoles of organosilica per gram of sample		
	Calculated by %C	Calculated by TGA	Calculated by ^{29}Si-NMR
SBA-15-APS	1.63	1.01	1.10
SBA-15-ABS	1.69	1.14	1.39
SBA-15-APhS	1.26	0.97	0.94

Sample	mmoles of C_{60} per gram of sample	
	Calculated by %C	Calculated by TGA
SBA-15-APS-C_{60}H	0.17	0.26
SBA-15-ABS-C_{60}H	0.24	0.31
SBA-15-APhS-C_{60}H	0.06	0.01

Table S2. Fitting parameters obtained by mathematical fitting of the cumulative release profiles of methylprednisolone from non-functionalized and functionalized mesoporous SBA-15 silica materials using first-order kinetic and Korsmeyer-Peppas drug release models. Beside the kinetic parameter values, the standard error is included.

Sample		First-order kinetic release model: $F(t) = F_o \cdot (1-e^{-k \cdot t})$			Korsmeyer-Peppas model: $f(t) = K \cdot t^n$		
		Y-axis intercept $Ln(F_o)$	Rate coefficient [min^{-1}]	R^2	Constant, K_{K-P}	Release exponent, n	R^2
SBA-15	pH 7.4	0.62±0.001	0.0080±0.0001	0.999	4.3±0.9	0.44±0.07	0.901
SBA-15-APS		1.44±0.05	0.0201±0.001	0.982	4.2±0.5	0.46±0.02	0.985
SBA-15-ABS		0.26±0.004	0.0034±0.001	0.990	1.7±0.2	0.54±0.02	0.990
SBA-15-APS-C_{60}H		0.55±0.02	0.0072±0.0005	0.970	4.3±0.4	0.43±0.03	0.985
SBA-15-ABS-C_{60}H		0.19±0.002	0.0045±0.0001	0.998	0.6±0.1	0.73±0.03	0.992
SBA-15-APS-C_{60}H	pH 4.6	0.29±0.002	0.0060±0.0001	0.998	1.2±0.1	0.53±0.02	0.993
SBA-15-ABS-C_{60}H		0.24±0.005	0.0090±0.0003	0.989	0.7±0.1	0.62±0.03	0.991

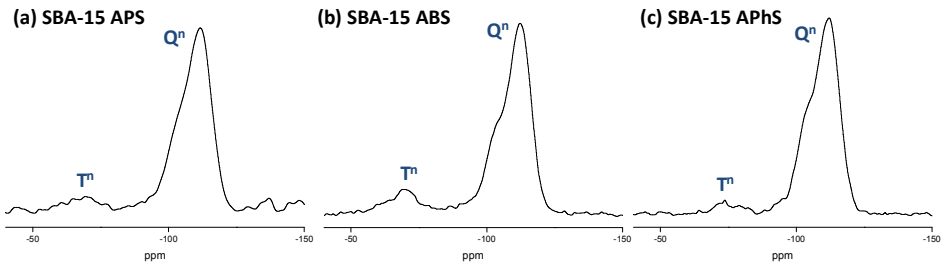

Figure S1. Solid-state 1D single-pulse ^{29}Si MAS NMR spectra of (a) SBA-15-APS, (b) SBA-15-ABS, and (c) SBA-15-APhS materials. Signals in a 1D single-pulse ^{29}Si NMR spectrum arise from chemically distinct ^{29}Si species and are resolved based on chemical shift, while their integrated areas reflect the quantities of each ^{29}Si species. Three distinct signals are observed at -110 and -102 ppm which are assigned to Q^4 and Q^3 ^{29}Si species, while the signals at ca. -65 ppm correspond to T^1, T^2, and T^3 ^{29}Si associated with amino organosilica species. The quantities of amino organosilica loadings are ascertained by comparing the integrated areas of signals from *T* and *Q* species reveal organosilica loadings (Table S1).

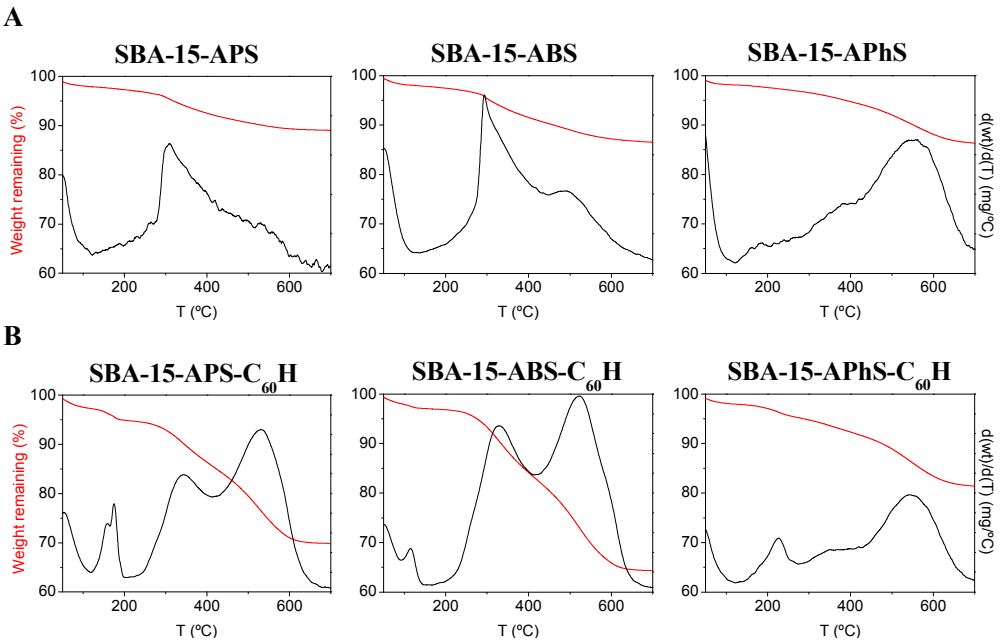

Figure S2. Thermogravimetric analyses plots of (A) SBA-15-NH_2 materials (B) SBA-15-NH-C_{60}H materials. The TGA plots of SBA-15-NH_2 materials (A) show mass losses between temperatures of 120 ºC and 700 ºC that are solely attributable to the decomposition of the organic moieties of amino organosilica species, and thus enable organosilica loadings to be quantified (Table S1). Additional mass losses are observed in the TGA plots of SBA-15-NH-C_{60}H materials (B) at temperatures of approximately 500 ºC, which are associated to the decomposition of fullerene C_{60} species. A comparison of mass losses between appropriate SBA-15-NH and SBA-15-NH-C_{60}H materials allows incorporated C_{60} species to be quantified (Table S1). In all TGA plots, mass losses between temperatures of 40 ºC and 120 ºC are attributed to the removal of adsorbed water.

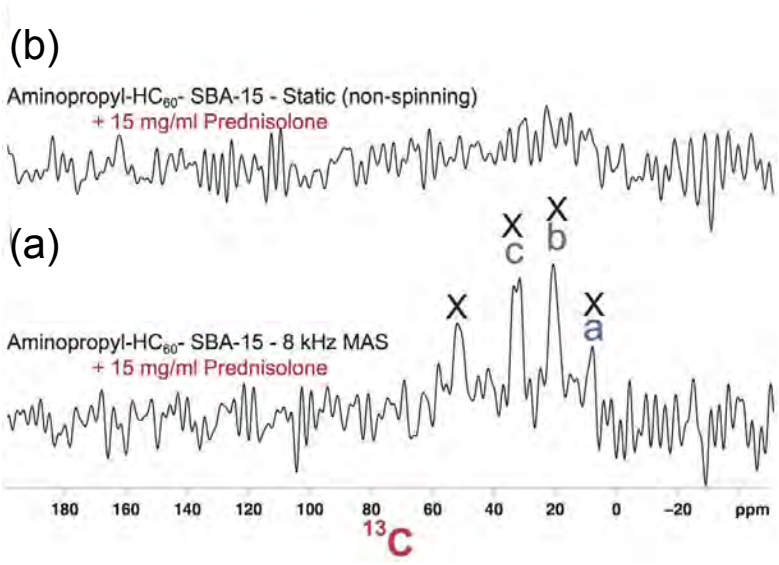

Figure S3. Solid-state 1D ^{13}C CP-MAS spectra of mesoporous SBA-15 silica functionalized with HC_{60}-aminopropyl groups with 15 mg mL^{-1} loadings of methylprednisolone guest species taken under (a) 8 kHz MAS and (b) static (non-spinning) conditions mg mL^{-1}. The spectra were all acquired at room temperature with a 2 ms CP contact time.

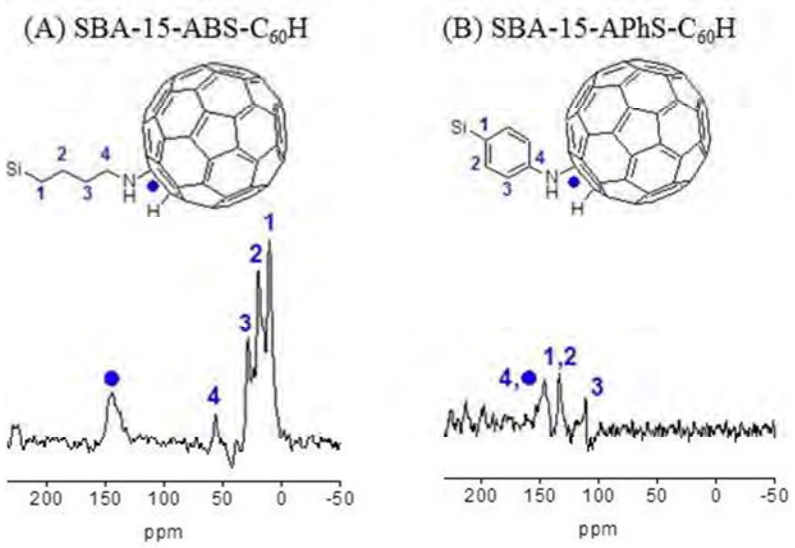

Figure S4. Solid-state 1D $^{13}C\{^{1}H\}$ CP-MAS NMR spectra of (A) SBA-15-ABS-$C_{60}H$ and (B) SBA-15-APhS-$C_{60}H$ materials. In A, ^{13}C signals at 11, 21, 29 and 57 ppm are assignable to ^{13}C species *1*, *2*, *3* and *4* of the aliphatic aminobutyl chains, while signals at *ca.* 145 ppm are attributable to the aromatic ^{13}C species of the C_{60} fullerene moieties. In B, the ^{13}C signals at 134 ppm are assignable to the aromatic ^{13}C groups *1* and *2*, while signals at 112 and 146 ppm are associated with ^{13}C species *3* and *4*, of the aminophenyl moieties of grafted aminophenyl organosilica species. Additionally, in B, the ^{13}C signals at *ca.* 145 ppm are associated with associated with the HC_{60} moieties and overlap with signals associated with species *4* of the aminophenyl moieties. Both spectra were acquired at room temperature under MAS conditions of 6 kHz with CP contact times of 1 ms.

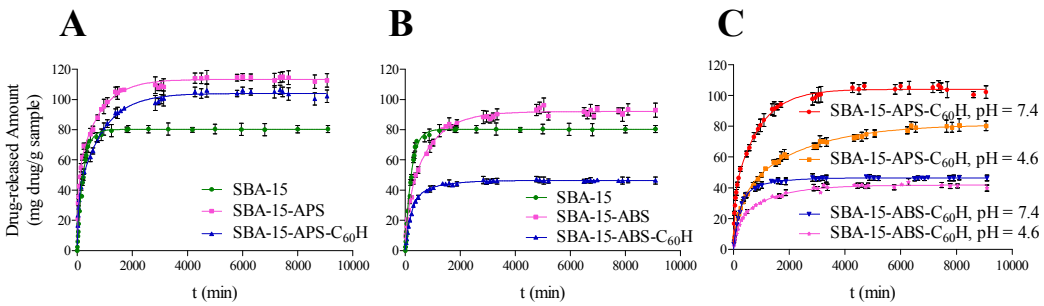

Figure S5. The cumulative profiles of methylprednisolone released into simulated body fluid (pH=7.4, 37 ºC) as a percent of the methylprednisolone adsorption capacity for a given material are plotted versus time for (A) SBA-15-APS (pink, squares) and SBA-15-APS-C_{60}H (blue, triangles) materials, and (B) SBA-15-ABS (pink, squares) and SBA-15-ABS-C_{60}H (blue, triangles). In (C), the extents of methylprednisolone released for SBA-15-APS-C_{60}H materials into simulated body fluids at pH 7.4 (red, circles) and pH 4.6 (orange, squares), and from SBA-15-ABS-C_{60}H into simulated body fluids at pH 7.4 (blue, triangles) and pH 4.6 (pink, stars) are plotted versus time. Simulated body fluid under approximately neutral conditions (pH 7.4) was a PBS buffered solution, while simulated body fluid under acidic conditions (pH 4.6) was an acetate buffered solution.

References

The complete author list of reference 34:

Uritu, C.M et al.; Varganici, C.D; Ursu, L; Coroaba, A; Nicolescu, A; Dascalu, A.I; Peptanariu, D; Stan, D; Constantinescu, C.A; Simion, V; Calin, M; Maier, S.S; Pinteala, M; Barboiu, M.